INTEGRATION OF LINEAMENT AND STRAIN ANALYSIS TO ASSESS LANDSLIDE VULNERABILITY ALONG TAIPING TO IPOH HIGHWAY, MALAYSIA

Idris Bello Yamusa[1,]* and Mohd Suhaili Ismail [2]
[1, 2] Geosciences Department, University Teknologi PETRONAS,
32610 Bandar Seri Iskandar, Perak, Malaysia;
[1] idris_18002911@utp.edu.my,
[2] suhaili.ismail@utp.edu.my,
* Correspondence: idris_18002911@utp.edu.my

Commission 4, WG 7

Abstract
The overall tectonics of a terrain and landslide occurrences can be controlled using lineament analysis. In addition, understanding the deformational characteristics of the rocks in question cannot be overemphasized. The current work was carried out along Taiping to Ipoh stretch of the North – South PLUS Highway Malaysia and its environs to assess landslide vulnerability via lineaments and strain deformation analysis. Approximately 73 km stretch of the road was analysed. Classification of about 197 lineaments was done from very high to very low density classes applying class break procedures to signify their respective risk zones. Fry strain analysis method was then integrated by digitizing the centre of the grains from which reference lines angles and axial ratios of 16 photomicrographs of various lithologies obtained from field investigations were used to understand their strain deformational pattern. The lineament intersection point map shows its concordance with the strain ellipsoid. The major trend of the lineaments and fry strain ellipsoid were both found to be trending NE–SW. Congruity between the lineaments intersection density and the flattened higher degree of strain signified a risk prone zone and probable landslide trigger along the highway.

Keywords – *Landslides, Highway, Lineaments, Deformation, Fry Strain*

1. Introduction

Generally, a rock slope collapse is disastrous; hence detection and stabilization should be done at the first phase. This is frequently necessary to avoid human life, vehicles, and infrastructure being lost as a result of the rock mass movement phases (Nagendran, ISMAIL et al. 2019). Building of highways, quarries and mining trenches create manmade rock slopes. In Malaysia, a number of the development operations were carried near unsteady rock slope faces (Abdullah, Rosle et al. 2015). These unsteady rock slope faces mostly lead to landslides. According to Georgiadis *et al.,* (Georgiadis, Tranos et al. 2007), the choice of a new road over an old is predicated on the actual fact that the old road segment that spans the rock formation, generating manmade slopes in diverse geological formations has variable mechanical properties, allowing for the assessment of various potential instabilities circumstances. It is therefore, necessary to cross check the security of a functioning road. Landslide management is focused on surface and geological studies, with relation to geomorphology and surface deformation (Wang, Schweizer et al. 2021). One among many of the means to tackle landslide problems is to examine the Lineaments which are expressions on the surface of weak regions or structural displacements of the earth’s crust (Abdullah, Nassr et al. 2013). Tectonic structures, landform features, or associated geologic features created naturally are related to the lineaments, which are straight or curved discontinuities in straight reference to the faults (Singh, Arya et al. 2020). Mapping these lineaments is not adequate by typical field techniques to provide a synoptic view. It necessitated the use of remote sensing data, which has shown to be a very useful tool recently.

Additionally, finite strain analysis techniques are utilised to numerically determine the amount of deformation in order to constrain the mechanics of the sliding sediment (Förster). Different methods of strain estimation, field observations and measurements are used to determine the strain intensity, direction of maximum elongation (σ_3) and compression direction (σ_1) (Oden, Ogunleye et al. 2015). By suggesting that measuring the deformation of sediments is a useful tool for comprehending the mechanics and slide evolution, Förster *et al.*, (Förster) connected the application of strain analysis to landslides. The Fry method was used to perform this as a useful tool to measure the strain ellipse from marker particles. It is advised that the results be accurate or amended by a computer programme that provides an automatically and objectively estimated strain ellipse. It is worthy of notice that the research was conducted on marine sediments and thus no information conveyed on lithological deformation of outcrops that may lead to landslides.

With regards to the current study, there is no literature on nature of rock deformation, there is unknown lineament density analysis along the highway, unknown relationship of hydrogeology with road network and vulnerability of Taiping to Ipoh segment of the Highway to hazards (Yusof, Pradhan et al. 2015).

Therefore, since interdisciplinary approach is recommended for landslide monitoring (Wunderlich 2006, Margottini, Bobrowsky et al. 2017, Gao, He et al. 2022, Saraskanrood and Piroozi 2022), and no research in documented globally on the proposed approach, the aim of this research is to Integrate lineament and strain analysis to assess landslide vulnerability along Taiping to Ipoh Highway, Malaysia by determining both the strain deformation type and pattern of rocks and the lineament intersection density of the study area and then correlating the points with both high strain deformation and high lineament intersection density as the most vulnerable zones to landslides occurrences.

1.1. Geology of Peninsular Malaysia

The Western to Eastern belts running from north–south (Fig. 1a) characterize the peninsula. Over Nine-Tenth (9/10) of Peninsular Malaysia plutonic rocs are granitic. The granitoids can be separated into two belts: the West Malaya Main Range and the East Malaya Main Range, which are S-Type granitoids from the Late Triassic to the Early Jurassic and I-Type granitoids ranging in age from the early Middle Permian to the early Late Triassic respectively. The Peninsula was impacted by a massive Late Cretaceous tectono-thermal event that resulted in severe faulting, granitoid intrusion, and resetting of palaeomagnetic signals (Metcalfe 2013). The study area also falls within the Western Belt of Peninsular Malaysia having a primary range Late Triassic to early Jurassic granitoids belonging to the S-type group. There are two sets of brittle fractures affecting the encompassing plutons one in all which should indicate the accommodation at two different structural depths of deformation and in relation to the cleavage is parallel (Sautter, Pubellier et al. 2017). Moreover, the geomorphology of the world consists of hilly terrains and undulating plateaus. Granite from the Quaternary and Devonian periods dominates the world's geology. Many landslides have been documented in recent years along PLUS highways, local roads and waterways that scrape the perimeters of watercourses (Yusof, Pradhan et al. 2015).

1.2. The Study Area

The Expressway running from North to South which is the longest highway in Malaysia stretching from Bukit Kayu Hitam to Johor Bahru (Fig. 1b) having a distance of around 772 km (Klia2.info 2019). Major towns and cities are connected by this highway therefore acting as pillar to industrial prosperity (Fig. 1c) Peninsular Malaysia(Ahmad, Zin et al. 2016). The study area (Fig. 3) which is the environs of the part North South Highway extends from Taiping at 4° 51' N and 101° 43' E of latitude and longitude respectively to Ipoh at 4° 35' N and 101° 04' E of latitude and longitude respectively, with a distance of around 73 km. Remarkably, some parts of the research area are subjected to frequent mass movements, which result in erosion and landslides. (Yusof, Pradhan et al. 2015).

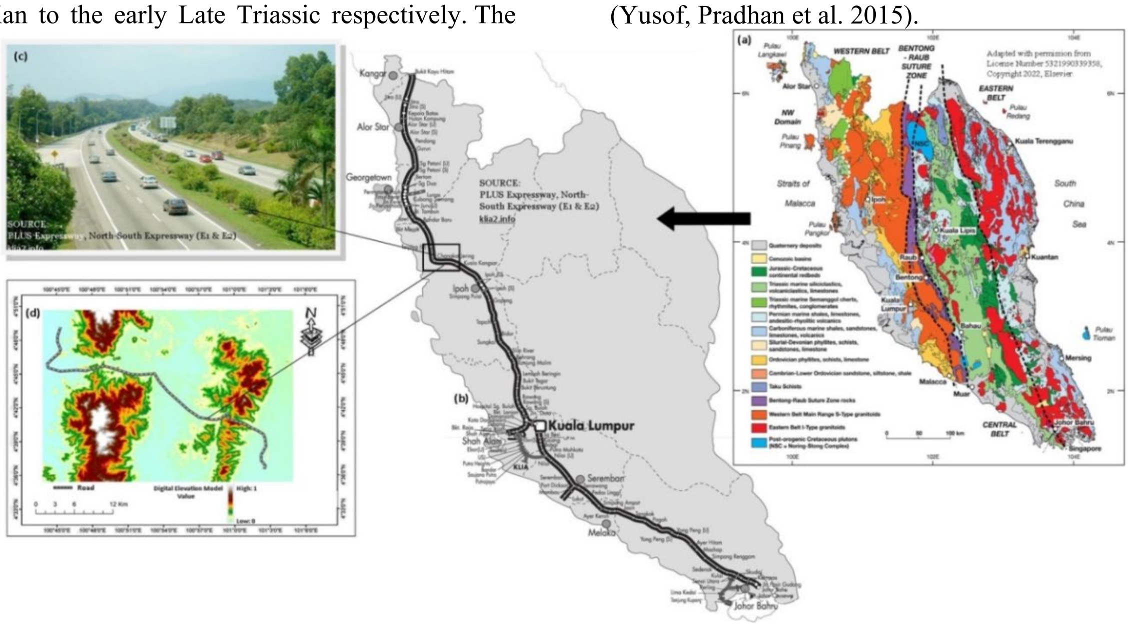

Figure 1: North-South PLUS Highway (a) Geological map of the Peninsula Malaysia, adapted from (Metcalfe 2013) with permission from License Number 5321990339358, Copyright 2022, Elsevier. (b) Location of Study area and connected major cities on the North-South Highway (c) Activeness and commercial importance of study area (d) Digital Elevation model showing the Highway segment under study.

2. Software and Methodology

A conceptual summary of methods used in the study is shown on Figure 2.

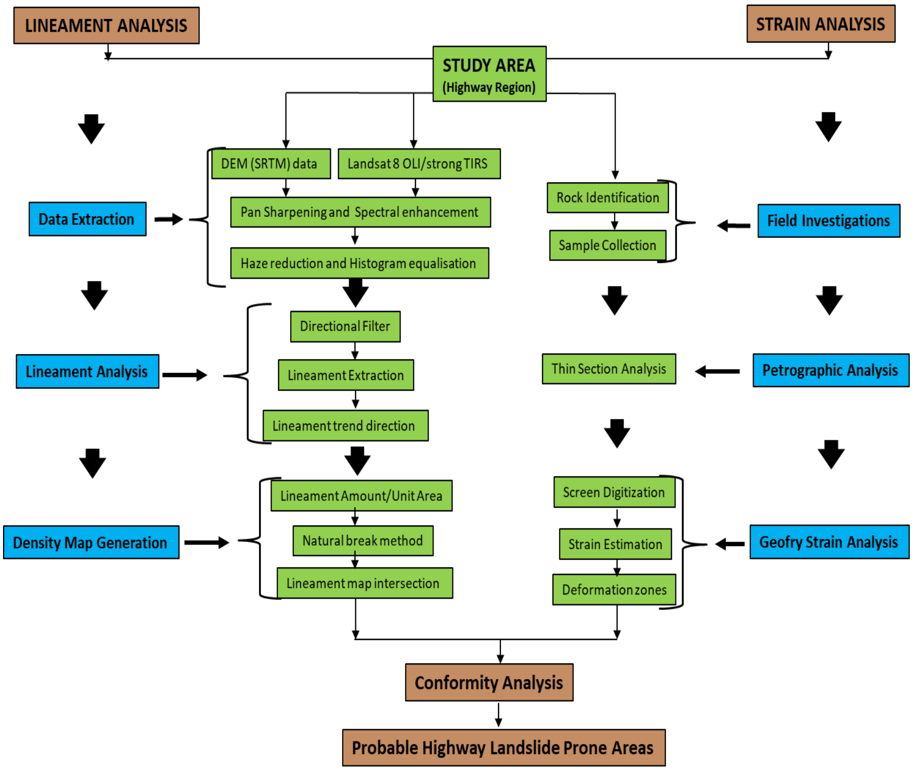

Figure 2: The scheme of the methodology of integrated research for landslides detection via Lineament and Strain Analysis

2.1 Lineament Analysis

The research area's Digital Elevation Model (DEM) was downloaded in Raster format from Shuttle Radar Topography Mission (SRTM) data (Fig 1d). It was then loaded into ArcGis 10.5 to extract the DEM and track the Highway section. The entire research region was covered by a Landsat 8 OLI/TIRS Level-1 C1 image obtained from www.earthexplorer.usgs.gov. 3D map layers Worldwide Reference System path and row are 127 and 057, respectively, and it was captured on February 20, 2021. The geographic resolution of the data is roughly 30 m, according to Singh et al. (Singh, Arya et al. 2020). The Landsat 8 OLI/strong TIRS's spectral bands combined with 30 m provide a significant benefit 30 m pixel size in OLI multispectral bands, OLI panchromatic bands 15 m and Thermal Infrared Sensor TIRS band 30 m pixel size. Satellite photos were processed using PCI geomatica 2015 software. The Pan Sharpen approach was utilised to lower the picture pixel size (Fig. 3) to 15 m, then Principal Component (PC) alongside spectral enhancement technique was employed to obtain a unique collection of data with better necessary information from the previous data collection.

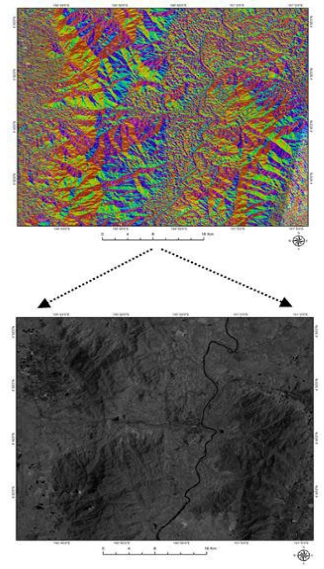

Figure 3: Satellite Image after mergence of principal component, pansharpened data and equalization of histogram.

In the radiometric processing, the haze reduction method and histogram equalisation were also used to improve the satellite images contrast. Removal of noise in the image is done with the noise reduction filter, and then the colour composition analysis is performed. Arc GIS 10.4.1 was used to create the secondary data and production of final maps of lineaments. The general trend lineaments were examined using the Rockworks-2015 software. The following stages describe the procedure for distinguishing lineaments from a processed satellite image:

2.1.1 Lineaments Extraction via Directional FilteringFor improvement of the features that are linear or curvilinear in the study area like the highway, faults or lithological boundaries and others, directional filter in PCI geomatica 2015 software is created. The convolution approach was used to apply a filter to which 3 x 3 high and low pass filters, enhancement of edge, reduction of haze and sharpening were applied. This filtration of image intensifies the spatial frequencies that are high in the data, emphasising the discontinuities of data [11]. Gradient filters were also applied in extraction the geological lineaments 3 x 3 Left, Right, Up and Down. There are also gradient filters used which are 3 x 3 horizontal, vertical and non-directional.. These filters improved the images-discontinuities parallel to the lineaments (Figs. 4 a and b).

2.1.2 Visual Lineaments Extraction The lineaments mapping is done by mapping all the linear characteristics on multiple images of Landsat 8 LI/TIRS C1 Level-1 that are filtered via application of directed filters, which is done depending on visual interpretations, picture quality, and study area complexity. To trace lineaments of geologic origin, evaluation of all lineaments traced are evaluated methodically via overlapping them with infrastructure (waterways, roads, etc.) and overlaying lineament maps gotten from diverse directions to create a combination lineament map. Lineaments that reappear more than once (Fig. 5a) were eliminated from the synthesis map to avoid recurrence. **2.1.3 Rose Diagram** To create the rose diagram, the dxf file was imported to a software Rockworks 15 for examination of lineament frequency and trend direction (Fig. 5b). For direction computation, the lineaments from their vertices are now separated into sections (Nath, Niu et al. 2017). The data management toolbox's split line at vertices tool was used to separate the lines, and then a lineament dxf file was created. ArcGIS 10.4.1 was used for all of the preceding methods.

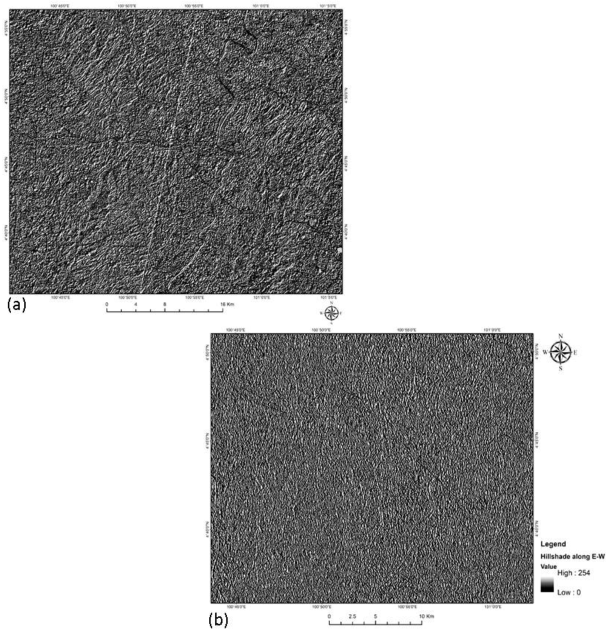

Figure 4: Satellite image Lineament acquired by directional filter, (a) lineaments oriented NE–SW with a trace of the Highway indicated (b) Hillshade along E-W.

2.1.4. Density Map Generation
To correctly monitor the state of the lineaments by the highway in relation to lineaments density, the density map was constructed by determining the lineaments amount for every unit area (Hung, Batelaan et al. 2005) using the spatial analyst in

https://doi.org/10.5194/isprs-archives-XLVIII-4-W6-2022-57-2023 | © Author(s) 2023. CC BY 4.0 License.

ArcGIS 10.4.1 software under line density tool. The resulting density map illustrates the collection of lineaments per unit area (Fig. 6a), which is subsequently divided into very low, low, moderate, high, and very high density classes. Applying the natural break method, the lineament map intersection was constructed by adding up all the locations of intersection of the lineaments extracted (Fig. 6b). The density and junction map of the lineaments were also compared to previously identified landslide locations (Yusof and Pradhan 2014, Singh, Arya et al. 2020).

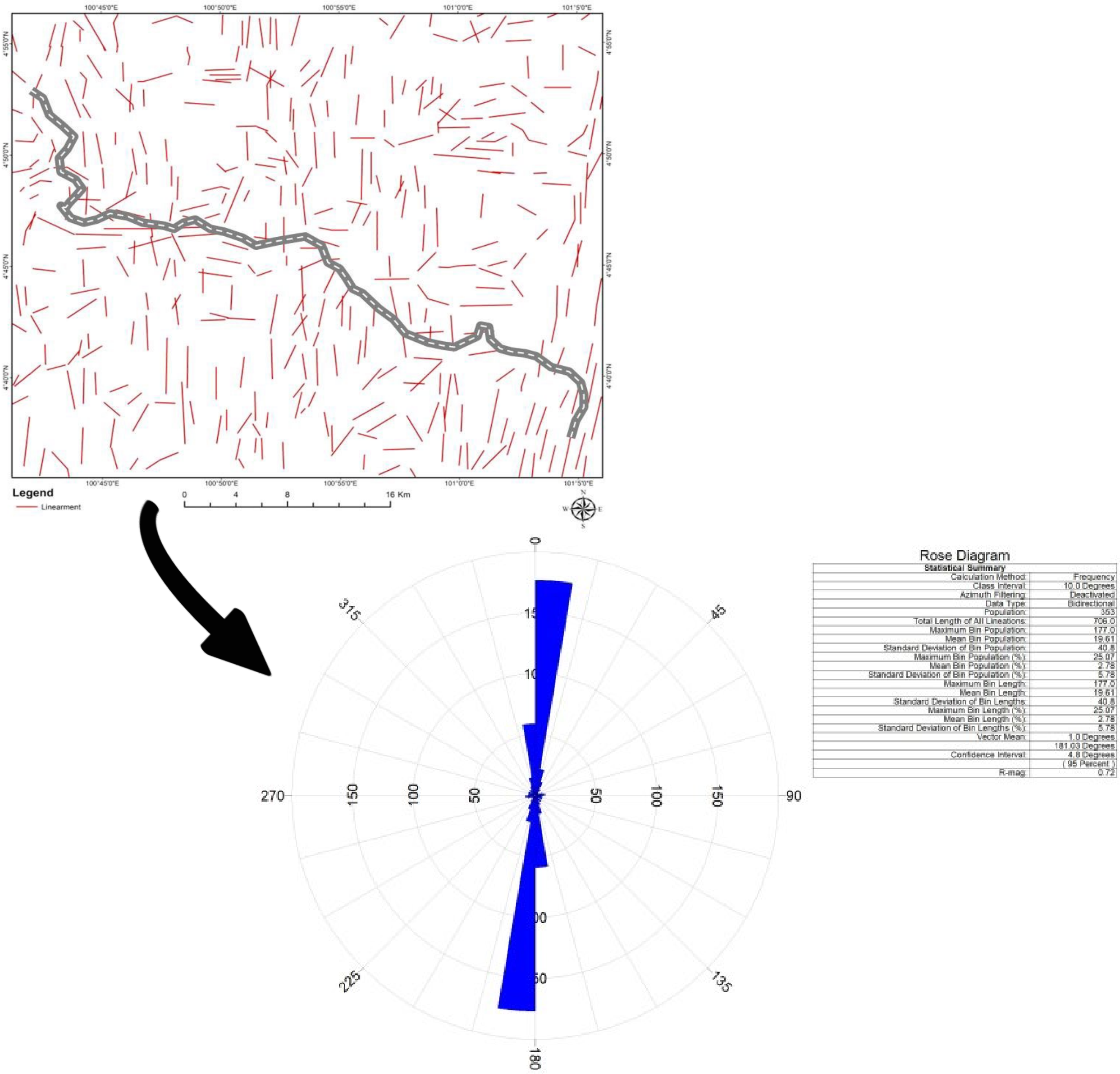

Figure 5: (a) Different directions of geological lineaments generated from satellite data (b) Lineament orientation showing prevalence of NE–SW directions acquired by different filters as shown in a rose diagram.

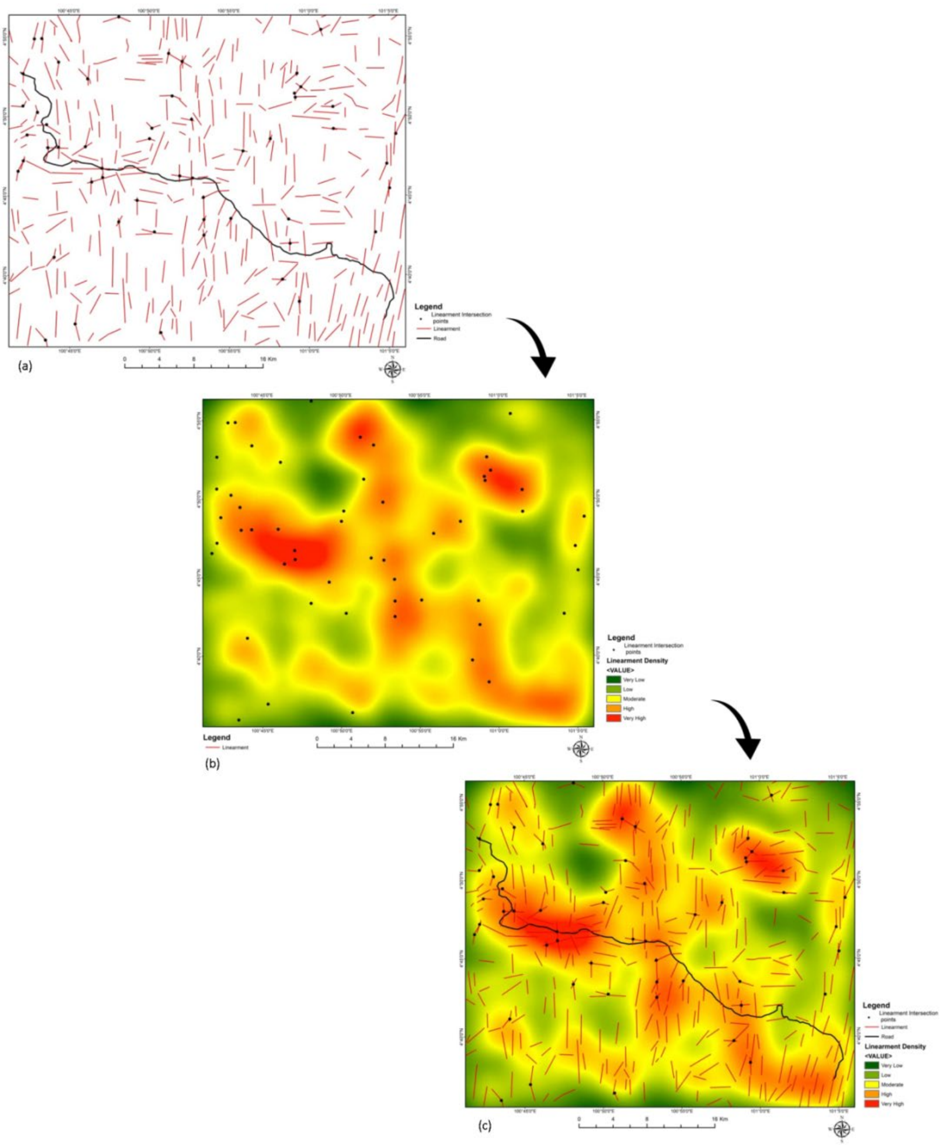

Figure 6: Lineament intersection maps (a) Showing crosscutting relationship with road under study (b) Showing Lineament density map and classes (c) Final output integrating lineament intersection and density map with road overlay.

2.2 Strain Analysis

The Fry (Fry 1979) method of strain analysis using a 2-D interactive geofry software plots using the Fry (1979) point-to-point method was used which is based on the hypothesis that an originally non-clustered distribution of points will change into an irregular distribution following deformation.

2.2.1. Field Investigations

The targets are the outcrops and slopes that failed along the North-South Highway about 73 Km. Type of lithology, coordinates of outcrops, geological structures, type and possible landslides to occur are the focus of the field investigation. Geological mapping method was done using GPS (the Global Positioning System) to track points on topographic map and take readings for required samples in specific locations. Description of the type of lithology, texture, grain size, roundness, sorting, fabric, structure) and mineral composition was attempted on the field. The petrographic analysis aims to determine the volumetric amount of the composition to determine precisely the name and rock texture, using the polarizing microscope (Cahyaningsih, Crensonni et al. 2018)

Seven (7) different locations were observed for sample collection and analysis (Table 2). Lithological constituents in the research area were classified as phyllites, shales and metasandstones in the North-western section of the research area. Fresh porphyritic granites covering more than 70% of the research area extending down to the southern part and limestone exposures down the soutfheastern part of the research area around Ipoh along with medium grained granite outcrops. Lineations which are the repeated, commonly penetrative and parallel alignment of linear elements were observed in the porphyritic granite. Arrays of elongate K-feldspar porphyroblasts were oriented with their long axis mutually parallel. The lineation is in the NNE-SSW direction (Fig. 7b). Cleavage represents the most conspicuous structural feature on the schists in the study area. It is defined by parallel splitting of the rock along preferred planes. It has a characteristic spaced cleavage having a major trend in a NNE-SSW direction and the trends are also shown on the rosette diagram (Fig. 7d).

2.2.2. Petrographic Analysis

Data processing phase consists of laboratory and analytical work in the studio. The analysis in the laboratory is petrographic analysis. While the analysis done in the studio include geological mapping, analysis of microstructures under a microscope and the percentage of grain composition is done by point counting method. Thin section of clastic sedimentary rocks encountered in the study area were classified using the classification of clastic sedimentary rock which makes the percentage of some components such as grains of quartz, feldspar, rock fragments, matrix (fine material) and cement solution

Table 2: Locations and coordinates of lithologies along the Taiping to Ipoh segment of the Highway

Locations	**Coordinates**	**Lithologies**
1	04° 32' 42.84" N 101° 02' 0.83" E	Medium Grained Granites
2	04° 36' 43.91" N 101° 02' 59.20" E	Sandstone
3	04° 37' 12.68" N 101° 03' 38.77" E	Medium Grained Granite
4	04° 58' 51.75" N 100° 38' 43.27" E	Shale, Weathered sandstone
5	04° 45' 27.69" N 100° 43' 51" E	Phyllites
6	04° 46' 27.75" N 101° 46' 41.20" E	Limestone (Inaccessible)
7	04° 46' 30.24" N 100° 38' 47.15" E	Porphyritic Granite
8	04° 38' 39.49" N 101° 05' 53.46" E	Limestone

At location 1 and 3, medium grained granite exposures were found to be relatively leucocratic (light brown) with pink coloured crystal of feldspar that lack clearly defined trend. At location 1, however, the rocks have been badly weathered and obtaining fresh sample was a bit difficult. Quartz was observed to be transparent and biotite occurs as black specks. In Plane Polarized Light (PPL), microcline has small bubbles referred to as granophyric intergrowth texture which is an intergrowth of quartz into plagioclase. Quartz has low relief, is colourless and has anhedral form The biotite is brown coloured with subhedral form and moderate relief. In Cross Polarized Light (XPL), microcline has grey interference colour and exhibits polysynthetic twinning (Fig. 7a). At location 2 Sandstone was observed but in a little exposure and only hand specimen was analysed. At location 4 phyllites are most typically seen as dispersed and worn remains with well-defined foliations oriented NE-SW, which are situated along a minor road going to Taiping. Field relationships demonstrate this type of older phyllites and shale as low-lying outcrops interbedded with heavily weathered sandstone in the peneplain in the northern half of the research region. They appear like microscopic lenses that have been thoroughly worn and are commonly visible near road cuttings. Phyllite (Fig. 7d) constitutes about 2% of the total rocks and has been affected by intense weathering so that fresh samples are difficult to obtain. In hand specimens, it is mostly dark grey to light brown in colour. It is generally fine grained. Biotite flakes are split into elongated clusters by light-colored material, which is usually quartz/feldspar crystals measuring millimetres to centimetres in size. In PPL, the quartz is colourless with low relief and brown lineated biotite is seen. The biotite displayed pleichroism from light to dark brown. Also, biotite grains show basal cleavage. In XPL, biotite mainly has brown interference colour.

At location 7, in hand specimens, the rock is generally grey in colour. In thin section, microcline phenocryst is clearly visible indicating the porphyritic nature of the rock. Biotite is brown and pleichroic from light to dark brown. In XPL, the biotite displayed brown interference colour. The biotite is seen to be altered to chlorite, hence the green colour. The orthoclase shows myremekitic intergrowth texture (Plate which is an intergrowth of quartz into orthoclase). Quartz in PPL is colorless but cloudy. At locations 6 and 8 limestone hills were located to be light coloured huge, of highly calcite composition and crystalline. Some were observed to have bedding of parallel layers (Fig 7c). This characteristic results in a very rough landscape with numerous crags, as seen at the mine site. At the limestone hills, alongside structural weak planes are solutions of the bedrock which has generated complex patterns of gorges, caves and collapsing structures noticed on the surrounding. Some of the caves often have large dimensions, taking the space of most of the interior of a hill (Zabidi, Termizi et al. 2016). The minerals of limestone have different forms such as anhedral and subhedral especially white limestone. The nature of growth in full minerals is completely crystalline, with a crystalloblastic texture, and certain minerals are granoblastic due to having lenticular shapes. In general, the degree of recrystallization is consistent. Calcite mineral dominates the thin section under study, which has a granoblastic texture. Calcite crystals are euhedral in form. Cleavage and symmetry extinction are visible. Quartz is anhedral in shape and has a first-order grey interference colour (Serge and Senthilkumar 2017).

https://doi.org/10.5194/isprs-archives-XLVIII-4-W6-2022-57-2023

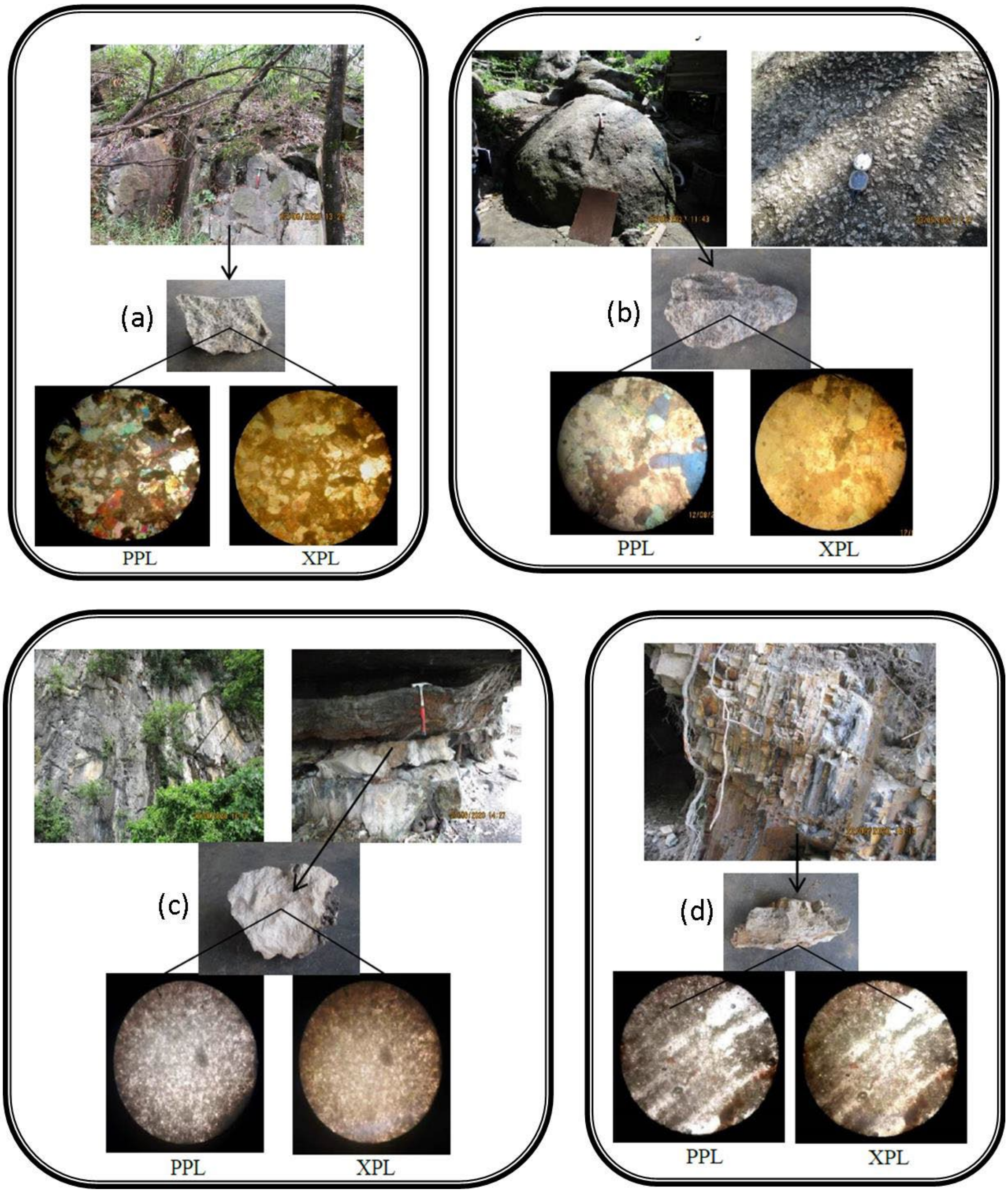

Figure 7: Petrograhy of Lithologies along Taiping to Ipoh Segment of the Highway showing outcrop exposures, hand specimens and thin sections in PPL and XPL of (a) Medium grained granite (b) Porphyritic granite (c) Limestone and (d) Phyllite

2.2.2. GeoFry Analysis

Sixteen (16) samples were employed for this analysis. Four (4) for the Medium grained granites, two (2) for the porphyritic granite, two (2) for the sandstone, two (2) for phyllite, four (4) for schist and two (2) for the limestone. Using the GeoFryPlots 3.1 software, by simply clicking the pointer on the centre of each grain which are porphyritic in the photomicrograph and creating a vacancy termed the Fry halo (Fig. 8) of ellipsoid forms, the short and long axes were digitised on selected micrographs of the rocks (Table 1). The strain ellipse's orientation was determined by the orientation of the ellipsoids. The flattened kind indicates a higher level of grain deformation, whereas the almost circular finite strain ellipsoid indicates a low level of grain deformation (Fig. 9).

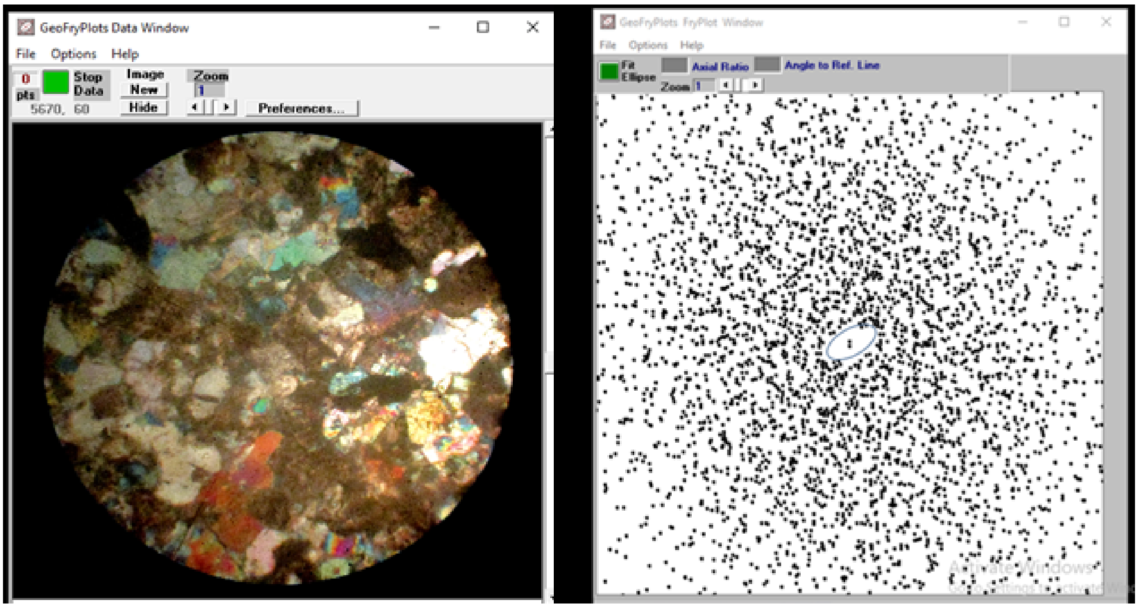

Figure 8: Digitization screen of Fry halos using GeoFryPlots 3.1 software

Table 1: Locations of obtained sample with respective ratios of their axes and reference line angles

S/N	Locations	Angle to Reference Line (degrees)	Axial Ratio
1	**L1**	**041**	**1.55**
2	**L1**	**038**	**1.57**
3	**L2**	**072**	**1.99**
4	**L2**	**056**	**1.83**
5	**L3**	**035**	**1.56**
6	**L3**	**032**	**1.90**
7	**L4a**	**083**	**1.86**
8	**L4b**	**072**	**1.72**
9	**L4c**	**065**	**2.12**
10	**L4d**	**062**	**2.15**
11	**L5**	**013**	**1.44**
12	**L5**	**016**	**2.32**
13	**L7**	**021**	**2.04**
14	**L7**	**031**	**2.41**
15	**L8**	**047**	**1.43**
16	**L8**	**035**	**1.65**

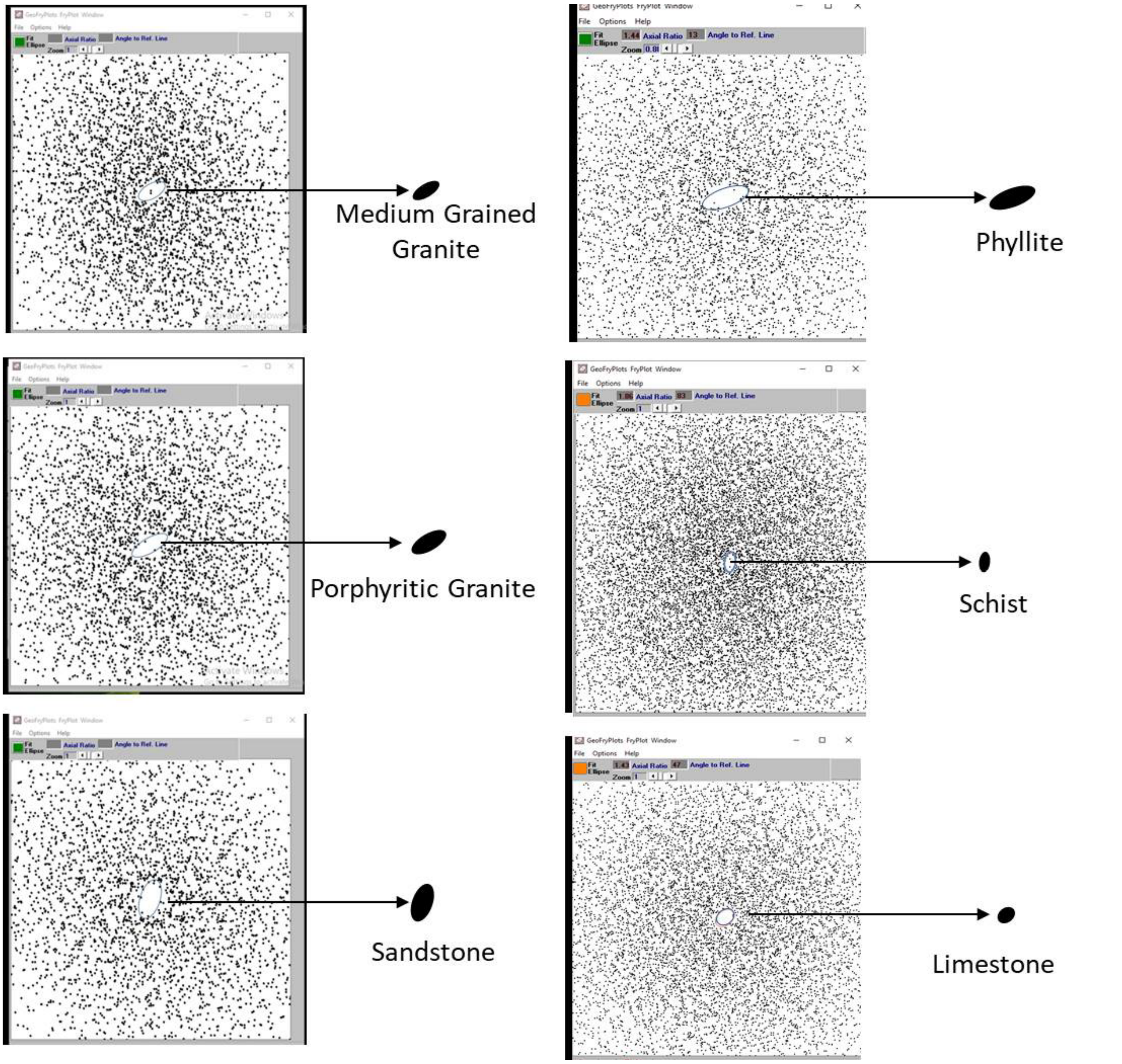

Figure 9: Fry halos obtained from respective samples within the study area.

3. Results and Discussions

New data containing very important information is produced via radiometric corrections and pan sharpening techniques. Lineaments and their frequencies were mapped in the research area by directional filtering which permitted the improvement of linear features. It is discovered that the majority of lineaments are oriented in the NE–SW, NW–SE, N–S, and E–W directions in that order subsequent to extraction of lineaments.

3.1 Geometrical Lineaments Analysis

This has been used to study the lineaments connectivity and recognised the main trend and tectonic condition of the research area, i.e., length, orientation and density. Geomorphological elements such as structural discontinuities are linked to the morphotectonics lineament study (Jordan and Schott 2005). Making orientation rosettes and total lineaments length to be proportional using classes of ten orientations is the typical method. The lineaments identified from the Landsat images are subjected to frequency analysis to emphasise on the main directions, which can then be compared by placing the lineament map with a drainage map. NE–SW and NW–SE directions are the main orientation of lineaments, with the former corresponding to the ductile deformation in the western belt of Peninsular

Malaysia, including upright folds which are non-symmetrical with axial surging. As a result, the NE–SW contractional strain vector impacted this area, followed by dextral shearing (Tjia 1989). In addition, Bok Bak NW–SE sinistral fault zone present to a degree in the western peninsular segment, and is among the largest faults in NW Peninsular Malaysia (Pour, Hashim et al. 2016). Hence, geometric analysis of the lineaments is a good technique in interpreting the tectonic orientation of the Highway research area.

3.2 Strain Estimation and Interpretation

For the strain analysis, sixteen (16) photomicrographs in total were utilized. The axial ratios, angle to the reference line, and the respective locations of samples (Table 1) were all recorded. The halo forms of the minerals created using the GeoFry software suggest heterogeneous deformation and varied grain orientations, primarily in the NE-SW axes. The Fry halo shapes along the highway range from near circular types in the southeastern parts of the highway cutting through the limestone region, implying a low level of deformation, to the non-circular oval shape in the northwestern segment of the highway near Taiping involving the metasedimentary region of phyllite outcrops, implying a high degree of deformation (Fig. 10b). The flattened spheroid shape of the Porphyritic granite outcrops was likely due to minor lineations of the plagioclase feldspar generated by shearing during deformation. The recorded strain inconsistency is owing to a difference in ductility across the different lithologies, which causes the lithologies to deform differently over the same deformation route. The halos were generally NE-SW, followed by NW-SE inclination. As a result, the strain cannot be linked to horizontal deformation or trends in the E-W to ENE-WSW axes (Umar, Danbatta et al. 2018).

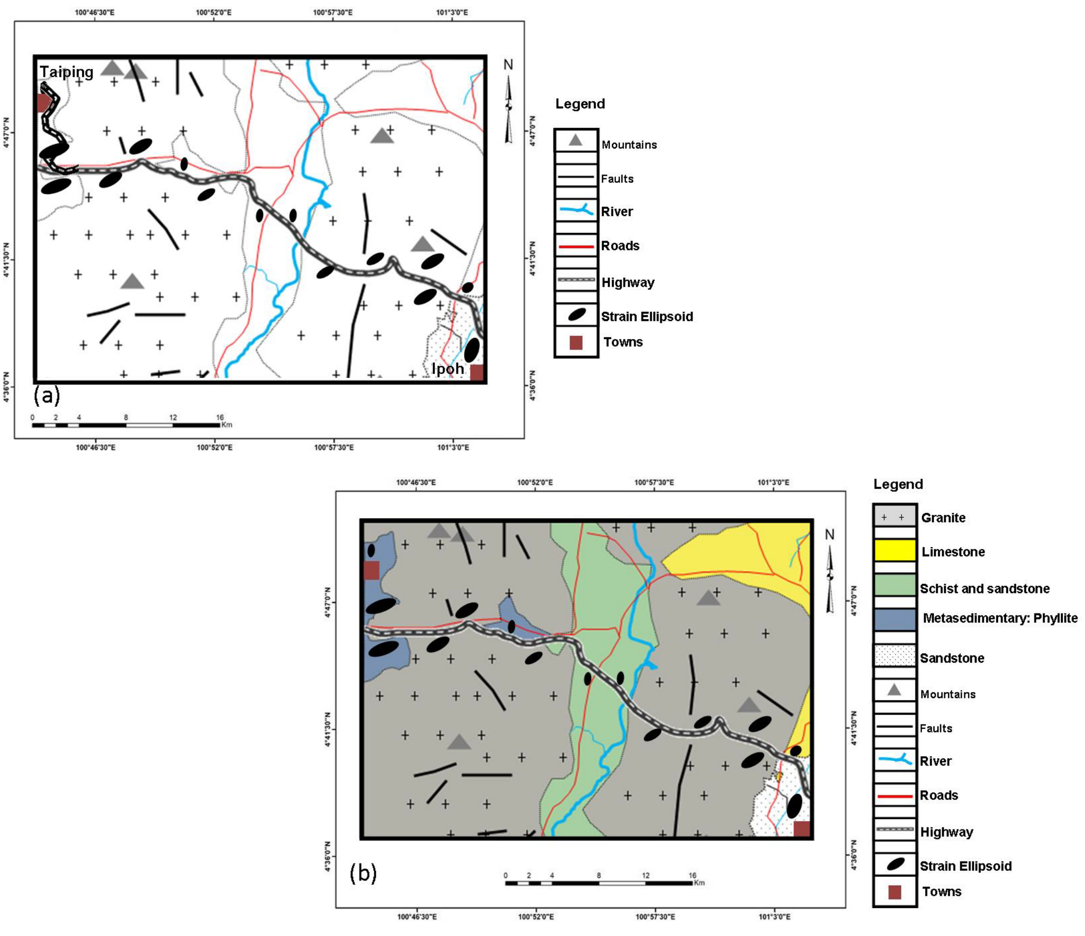

Figure 10: (a) The study area's map showing strain ellipsoid and orientation division (b) Orientation division and Strain ellipsoid map overlaid on geological map of study area.

3.3 Drainage Map

Water according to Sahu *et al.,* (Sahu and Dewangan 2018) is one of the causes of rock failures, therefore the corridors along the Highway was investigated for groundwater potential zones. The drainage map was created using a Cartosat DEM, which aids in determining the connection between patterns of lineaments and drainages. When the drainage and lineament maps were merged, it was discovered that a few of the major lineaments follow the same pattern of stream channel, indicating that these watercourses are manoeuvred structurally. The Drainages (Fig.11) are significant parameters in structural tectonic studies as they are prone to any tectonic changes (Singh, Arya et al. 2020). The streams follow the area's general regional topography; if they display any type of divergence (decapitated character) along their slope, it suggests a link between geo-structural elements of tectonic activity in the river course, such as the presence of lineament, faults, and so on. The fact that the drainage networks can be highly influenced by regional tectonics is confirmed by this change in the pattern of drainage in relation to the lineaments. In the research area, the pattern of the drainage shows anomalies which indicated the variance in tectonic activity that occurred in the area. The potential triggering mechanisms in the case of the highway region are complex hydro-geologically. Loss of the shear strength and dissolution may be caused by overpressure, seepage forces and increasing pore water pressure. Furthermore, the deformation characteristics such as high elasticity of rocks could highly favor the occurring of landslides. Inner erosion is not expected due to high percentage of granite in the study area and may erode quite slowly in such a tectonic non glacial climatic region. High precipitation may trigger superficial slides and flows whereas in the southeastern environs of the research area the limestone may act as sink for the groundwater (Brönnimann 2011).

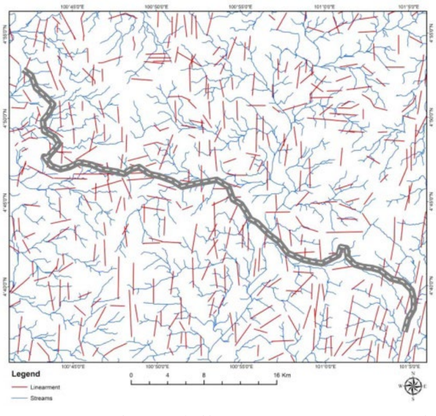

Figure 11: Overlay of lineament map on drainage map with position of Highway indicated

3.4 Conformity of Lineament and Strain Analysis in Landslide Vulnerability Corroboration

Density maps or the number of lineaments per unit area have been divided using the natural break method into very low, low, moderate, high and very high. Creation of lineament intersection map was done, and it depicts the highest incidence of lineament occurrence in areas with high lineament density (Fig. 6). With respect to deformation, it was indicated that the north-western belt of Peninsular Malaysia which the study area falls within, suffered the worse deformation than the other places (Omar 2010). The deformation characteristics of a rock must be known in order to determine the strain in the rock. Since most granitic rocks display orthotropic deformation on the assumption that when exposed to hydrostatic stress a circle of anisotropic material will distort into an ellipse and a sphere will distort into an ellipsoid (Farrow 1973). Deformation causes by the main stresses in rocks are mutually perpendicular, with σ_1, σ_2, and σ_3 being the largest, intermediate and maximum compressive stresses and maximum tensile stress (least compressive stress) respectively (Anderson 1937). As Indicated by Kinematics of Strain and associated stress patterns with respect to the tectonic structure of the study area (Fig.12), strain ellipsoid data from the various locations within the highway suggests minimum principal stress that is aligned NE-SW and maximum principal .stress that is aligned NW - SE (Solomon and Ghebreab 2006). Delicately, the orientation on landslides is apparently influenced profoundly by that of crustal stresses (Ai and Scheidegger 1984), on slopes which are perpendicular to the minimum tensile stress σ_1, head scarps tend to be regular while in concordance with the maximum horizontal tensile stress σ_2 or σ_3 mass movements incline to take place (Scheidegger and Ai 1986, Alexander and Formichi 1993). According to Sautter *et al.,*(Sautter, Pubellier et al. 2017) the region of study has tectonic influence as evident from granite plutons' conjugate pairs of fractures which were NE-SW and NW-SE. The N-S normal faults could be seen at a local or regional scale. On the respected lithologies along the highway, the ellipsoid was practically circular, indicating a low level of deformation, and non-circular or oval shaped, suggesting a greater degree of grain deformation. The halos were generally NE-SW, followed by the NW-SE inclination.

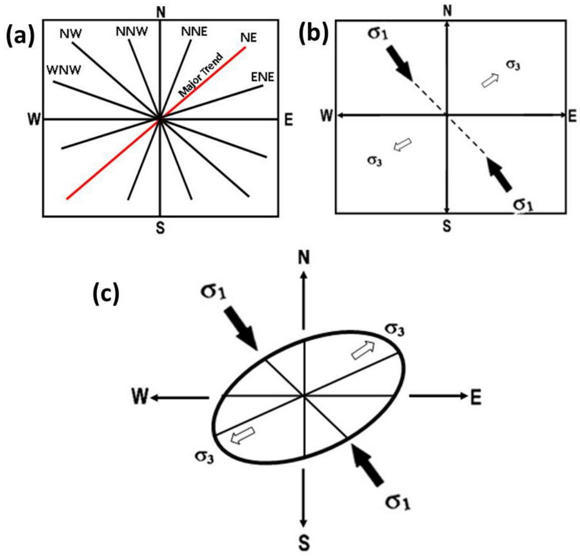

Figure 12: Kinematics of Strain and associated stress patterns with respect to the tectonic structure of the study area with emphasis on the two phases of deformational ellipsoid (a) Different orientations, with the NE–SW fractures as the major trend, (b) the trends of the main stress axes $\sigma_1 - \sigma_3$ (c) integrated kinematic strain analyses indicating deformational ellipsoidal trend Modified from (Solomon and Ghebreab 2006).

The density and intersection map overlap with the strain ellipsoids in the corresponding locations interpret the association between lineaments and regional deformation. Since in the high classes of lineament intersection density, high degree of flattening of the ellipsoid was observed indicating intensive deformation and also in the closeness of lineament zones of intersection, this suggests their origination from tectonism (Singh, Arya et al. 2020). The majority of the reported flat stain ellipsoid falls within the closeness of lineament zones of intersection and lineament density regions that are high along the highway, implying a tectonically active study area based on the density and intersection maps of lineament (Fig. 12). In addition, based on the correspondence of geological map with extracted lineaments, most of the lineaments were observed to follow the NE–SW trend which also conforms with the major direction of the strain halos in this region (Figs. 4b and 12). The structural mapping of Malaysia's western Bentong-Raub Suture Zone follows similar tectonic pattern (Pour, Hashim et al. 2016). The zones of intersections of lineaments are inferred to be tectonically active due to their intersections at different locations and existence of high number of lineaments, which leads to the slope discontinuity weakness and could additionally result in rock failure as reported in some parts of the highway environs (Yusof and Pradhan 2014). Ultimately, the synchronicity between the lineaments intersection density and the flattened higher degree of strain signified a risk prone zone to landslides, and the severinity of incentives and rock strength within a regional scale control the distribution of landslides (Chen, Chang et al. 2019).

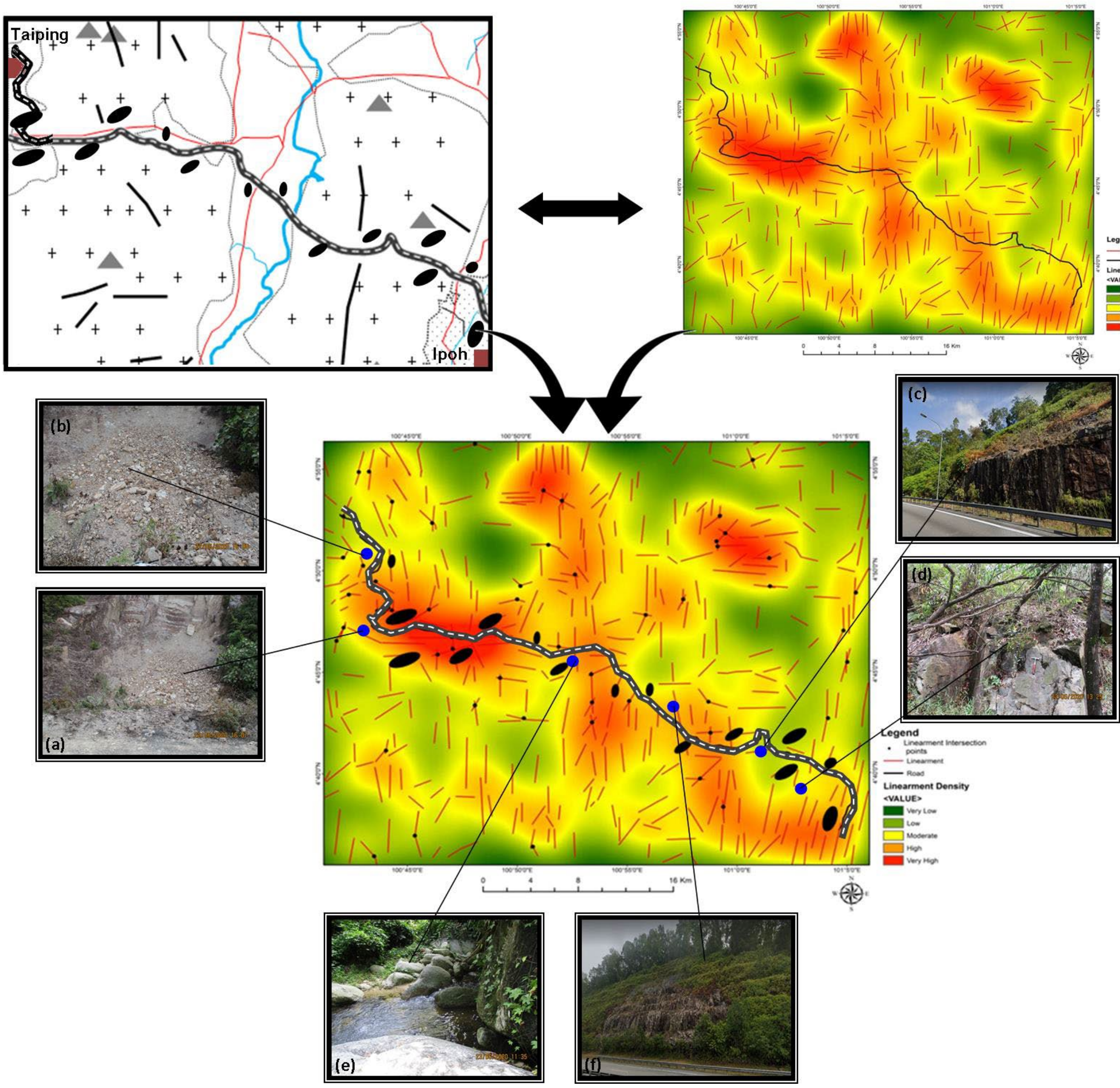

Figure 13: Superimposition of lineament thematic map over strain ellipsoid and orientation distribution map indicating landslide vulnerability with respective ground truthing conducted verifying each of the lineament density classes.

Evidence from field work carried out confirms the accuracy of the present mapping results on a qualitative level. Figure 13 shows the landslide vulnerability map generated through combination of strain ellipsoid and orientation distribution map with lineament density and intersection map. The integrated vulnerability map is classified into five: very low, low, moderate, high, and very high. The road that stretches from Taiping to Ipoh is overlaid across the map. It is observed that the highway is prone to landslide considering that it is mainly overlaid on the high to very high susceptibility to landslide. According to Yusof *et al.*(Yusof, Pradhan et al. 2015), several landslides have been reported along the PLUS highway road. Construction of roads based on geological mapping and hazards research findings will help reduce construction costs and ensure safety. Ground Truthing conducted (Fig. 13) verifies each of the lineament density vulnerability classes. The regions with high lineament density and vulnerability are seen to exhibit high weathering and partial landslides with unstable lithologies (Figs 13a and b) while regions with low to medium lineament density and vulnerability classes are seen to have stable rocks and boulders without any partial landslides (Figs 13c and d). Nevertheless, some few granitic areas of the highway with superficial stable rocks fall under the medium to high density classes of lineament and vulnerability (Figs 13 e and f), indicating they are worthy of additional investigation using a different approach.

4. Conclusion

Distinct major and minor lineaments via edge detection processes have been inferred to be useful in comprehending the pattern of tectonics in study area and predictive landslide analysis. The examination of the lineament density suggests that majority of the lineaments observed in satellite images are impressions of geological facets. Deformations have occurred in the area, as evidenced by drainage deviation, high density regions of lineaments and their intersections by the highway. The majority of lineaments are oriented in the NE–SW direction, followed by the NW–SE direction, N–S, and E–W directions. The current research does signify that lineaments are the grounds and stimulus for the possible occurrence of landslides in the study area along the Highway. Furthermore, this research establishes a relationship and improved understanding between lineament and the deformational history with regards to landslide vulnerability detection. The area's long axes of strain are mostly inclined in the NE-SW trending directions, which coincide with the lineaments. Changes in the magnitude and orientation of halos reveal heterogeneity in the bulk strain, which can be related to differences in mineral assemblages and metamorphic processes across the research area.

Finally, combining these two different tectonic analyses and congruity between them signifies risk prone zones of weaknesses and a probable landslide triggers along the highway which disaster management authorities should look into.

Funding

This research did not receive any specific grant from funding agencies in the public, commercial, or not-for-profit sectors.

Competing Interest

The authors affirm that they have no known financial or interpersonal conflicts that would have appeared to have an impact on the research presented in this study.

Acknowledgment

The authors of this article would like to thank the Department of Geoscience Universiti Teknologi PETRONAS and the University at large for the necessary support and assistance to undertake and complete this write up.

References

Abdullah, A., S. Nassr and A. Ghaleeb (2013). "Remote Sensing and Geographic Information System for Fault Segments Mapping a Study from Taiz Area, Yemen." Journal of Geological Research.

Abdullah, R. A., Q. A. Rosle, M. Al-Bared, N. H. Haron, M. Kamal and M. Ghazali (2015). Stability assessment of rock slope at pangsapuri intan, cheras. International Conference on Slopes Malaysia. 14th–16th Sept.

Ahmad, A. C., I. N. M. Zin, M. N. Rosli, A. M. Ab Wahid and I. F. M. Kamar (2016). Hazard and Risk of Highway Maintenance Works: Case Study of PLUS Expressways. MATEC Web of Conferences, EDP Sciences.

Ai, N. and A. Scheidegger (1984). On the connection between the neotectonic stress field and catastrophic landslides. Proceedings of the 27th International Geological Congress, Moscow.

Alexander, D. and R. Formichi (1993). "Tectonic causes of landslides." Earth Surface Processes and Landforms **18**(4): 311-338.

Anderson, E. M. (1937). "IX.—the dynamics of the formation of cone-sheets, ring-dykes, and caldron-subsidences." Proceedings of the Royal Society of Edinburgh **56**: 128-157.

Brönnimann, C. S. (2011). Effect of groundwater on landslide triggering, EPFL.

Cahyaningsih, C., P. F. Crensonni, Y. Aditia, A. Suryadi, Y. Yuskar, T. Choanji and D. B. E. Putra (2018). "Petrography, Geology Structure and Landslide Characterization of Sumatra Fault Deformation: Study Case In Km 10-15 Highway, Koto Baru Sub District, West of Sumatra." Journal of Geoscience, Engineering, Environment, and Technology **3**(4): 192-199.

Chen, Y. C., K. T. Chang, S. F. Wang, J. C. Huang, C. K. Yu, J. Y. Tu, H. J. Chu and C. C. Liu (2019). "Controls of preferential orientation of earthquake- and rainfall-triggered landslides in Taiwan's orogenic mountain belt." Earth Surface Processes and Landforms **44**(9): 1661-1674.

Farrow, R. A. (1973). A new method for the determination of three-dimensional deformation anisotropy in rock specimens, US Government Printing Office.

Förster, A. "Finite strain analysis in marine landslide sediments."

Fry, N. (1979). "Random point distributions and strain measurement in rocks." Tectonophysics **60**(1-2): 89-105.

Gao, H., L. He, Z.-w. He and W.-q. Bai (2022). "Early landslide mapping with slope units division and multi-scale object-based image analysis—A case study in the Xianshui river basin of Sichuan, China." Journal of Mountain Science **19**(6): 1618-1632.

Georgiadis, G., M. Tranos, T. K. Makedon and G. C. Dimopoulos (2007). "Contribution of geological mapping in road construction: an example from Verta-Kozani National road, Kastania area." Bulletin of the Geological Society of Greece **40**(4): 1652-1663.

Hung, L., O. Batelaan and F. De Smedt (2005). Lineament extraction and analysis, comparison of LANDSAT ETM and ASTER imagery. Case study: Suoimuoi tropical karst catchment, Vietnam. Remote sensing for environmental monitoring, GIS applications, and geology V, International Society for Optics and Photonics.

Jordan, G. and B. Schott (2005). "Application of wavelet analysis to the study of spatial pattern of morphotectonic lineaments in digital terrain models. A case study." Remote Sensing of Environment **94**(1): 31-38.

Klia2.info (2019). "PLUS Expressway, North-South Expressway (E1 & E2) ".

Margottini, C., P. Bobrowsky, G. Gigli, H. Ruther, D. Spizzichino and J. Vlcko (2017). Rupestrian world heritage sites: instability investigation and sustainable mitigation. Workshop on World Landslide Forum, Springer.

Metcalfe, I. (2013). "Tectonic evolution of the Malay Peninsula." Journal of Asian Earth Sciences **76**: 195-213.

Nagendran, S. K., M. ISMAIL, M. ASHRAF and W. Y. TUNG (2019). "Integration of UAV photogrammetry and kinematic analysis for rock slope stability assessment." Bulletin of the Geological Society of Malaysia **67**.

Nath, B., Z. Niu, S. Acharjee and H. Qiao (2017). "Monitoring the geodynamic behaviour of earthquake using Landsat 8-OLI time series data: case of Gorkha and Imphal." Natural Hazards and Earth System Sciences Discussions: 1-26.

Oden, M. I., P. O. Ogunleye and E. Udinmwen (2015). "Measurement of Pan-African strain in Zaria Precambrian granite batholith, northwestern Nigeria." J App Geol Geophys **3**(1): 21-30.

Omar, K. M. (2010). "Crustal deformation study in Peninsular Malaysia using global positioning system."

Pour, A. B., M. Hashim, C. Makoundi and K. Zaw (2016). "Structural mapping of the Bentong-Raub suture zone using PALSAR remote sensing data, Peninsular Malaysia: implications for sediment-hosted/orogenic gold mineral systems exploration." Resource Geology **66**(4): 368-385.

Sahu, K. C. and P. K. Dewangan (2018). Mixing of Fly Ash with Coal Mine Overburden to Increase the Slope Stability.

Saraskanrood, S. a. and E. Piroozi (2022). "Comparative evaluation of WLC, OWA, VIKOR, and MABAC multi-criteria decision-making methods in landslide risk zoning

Case study: Givi-chay watershed of Ardabil province." Journal of Physical Geography Research **54**(1).

Sautter, B., M. Pubellier, P. Jousselin, P. Dattilo, Y. Kerdraon, C. M. Choong and D. Menier (2017). "Late Paleogene rifting along the Malay Peninsula thickened crust." Tectonophysics **710**: 205-224.

Scheidegger, A. E. and N. Ai (1986). "Tectonic processes and geomorphological design." Tectonophysics **126**(2-4): 285-300.

Serge, N. and G. Senthilkumar (2017). "Petrography Of Crystalline Limestone And The Associated Rocks Occurred Near Uthappanaickanoor Village, Usilampatti Block, Madurai District, Tamil Nadu, India."

Singh, K., A. K. Arya and K. K. Agarwal (2020). "Landslide Occurrences Along Lineaments on NH-154A, Chamba, Himachal Pradesh; Extracted from Satellite Data Landsat 8, India." Journal of the Indian Society of Remote Sensing **48**: 791-803.

Solomon, S. and W. Ghebreab (2006). "Lineament characterization and their tectonic significance using Landsat TM data and field studies in the central highlands of Eritrea." Journal of African Earth Sciences **46**(4): 371-378.

Tjia, H. (1989). "Tectonic history of the Bentong-Bengkalis suture."

Umar, A., U. Danbatta and T. Najime (2018). "Application of Fry Strain Analysis Technique on Metasediments Arround Danko Area, Sheet 74sw, Part of Zuru Schist Belt, Northwestern Nigeria." J Geol Geophys **7**(332): 2.

Wang, J., D. Schweizer, Q. Liu, A. Su, X. Hu and P. Blum (2021). "Three-dimensional landslide evolution model at the Yangtze River." Engineering Geology **292**: 106275.

Wunderlich, T. (2006). Geodätisches Monitoring–ein fruchtbares Feld für interdisziplinäre Zusammenarbeit. VGI-Österreichische Zeitschrift für Vermessung & Geoinformation.

Yusof, N. M. and B. Pradhan (2014). Landslide susceptibility mapping along PLUS expressways in Malaysia using probabilistic based model in GIS. IOP Conference Series: Earth and Environmental Science, IOP Publishing.

Yusof, N. M., B. Pradhan, H. Z. M. Shafri, M. N. Jebur and Z. Yusoff (2015). "Spatial landslide hazard assessment along the Jelapang Corridor of the North-South Expressway in Malaysia using high resolution airborne LiDAR data." Arabian Journal of Geosciences **8**(11): 9789-9800.

Zabidi, H., M. Termizi, S. Aliman, K. Ariffin and N. Khalil (2016). "Geological structure and geomorphological aspects in Karstified susceptibility mapping of limestone formations." Procedia Chemistry **19**: 659-665.